



Numerical Analysis and Prediction of Unsteady Forced Convection over a Sharp and Rounded Edged Square Cylinder

P. Dey[†] and A. Das

Department of Mechanical Engineering National Institute of Technology Agartala, India

[†]Corresponding Author Email: prasenjitmit1@gmail.com

(Received October 13, 2014; accepted April 15, 2015)

ABSTRACT

An unsteady two-dimensional forced convection over a square cylinder with sharp and rounded corner edge is numerically analyzed for the low Reynolds number laminar flow regime. In this study, the analysis is carried out for Reynolds number (Re) in the range of 80 to 180 with Prandtl number (Pr) variation from 0.01 to 1000 for various corner radius ($r=0.50, 0.51, 0.54, 0.59, 0.64$ and 0.71). The lateral sides of the computational domain are kept constant to maintain the blockage as 5%. Heat transfer due to unsteady forced convection has been predicted by Artificial Neural network (ANN). The present ANN is trained by the input and output data which has been acquired from the numerical simulation, performed in finite volume based Computational Fluid Dynamics (CFD) commercial software FLUENT. The heat transfer characteristics over the sharp and rounded corner square cylinder are evaluated by analyzing the local Nusselt number (Nu_{local}), average Nusselt number (Nu_{avg}) at various Reynolds number, Prandtl numbers and for various corner radii. It is found that the heat transfer rate of a circular cylinder can be enhanced by 12% when Re is varying and 14% when Prandtl number is varying by introducing a new cylinder geometry of corner radius $r=0.51$. It is found that the unsteady forced convection heat transfer over a cylinder can be predicted appropriately by ANN. It is also observed that the back propagation ANN can predict the heat transfer characteristics of forced convection very quickly compared to a standard CFD method.

Keywords: Square cylinder; Rounded corner; Forced convection; ANN.

NOMENCLATURE

B	blockage ratio	x, y	Cartesian coordinates
C _p	specific heat of the fluid	R	radius of rounded corner
D	width of the square cylinder	r	radius of rounded corner
h	local convective heat transfer coefficient	u, v	velocity components in x and y directions
H	height of the domain	μ	viscosity of the fluid
k	thermal conductivity of the fluid	ρ	density
L _d	downstream boundary distance from the cylinder center	θ	Dimensionless temperature
L _u	upstream boundary distance from the cylinder center	Subscript	
Pr	prandtl Number	∞	free stream
Re	Reynolds Number	w	cylinder surface
t	time	Superscript	
U _∞	free stream velocity	-	dimensional variable

1. INTRODUCTION

Over the last many years, the flow and heat transfer around slender cylindrical bluff bodies has been the subject of intense research, mainly owing to the tremendous engineering significance on heat exchangers, solar heating systems, natural

circulation boilers, nuclear reactors, dry cooling towers, electronic cooling, vortex flow meters and flow dividers, probes and sensors and many more. Even though there is no information available in the literature about the heat transfer around obstacles with a square cylinder of rounded corner edges at low to moderate Reynolds number.

The vast majority of these studies have been carried out for the flow and heat transfer investigation past a circular cylinder, sharp-edged square and triangular cylinder. Based on a combination of numerical, theoretical and experimental studies, different flow regimes for the square cylinder have been identified in the literature depending upon the value of the Reynolds number and Prandtl number (A. Sohankar, 1995; Bhattacharyya and Mahapatra, 2005; Breuer, Bernsdorf, Zeiser, and Durst, 2000; Dhiman, Chhabra, and Eswaran, 2005; Dhiman, Chhabra, Sharma, and Eswaran, 2006; Gupta, Sharma, Chhabra, and Eswaran, 2003; Ji, Kim, and Hyun, 2008; Rahnama and Hadi-Moghaddam, 2005; Sahu, Chhabra, and Eswaran, 2009; Sharma and Eswaran, 2004a, 2004b; Sheard, Fitzgerald, and Ryan, 2009; Sohankar, Norberg, and Davidson, 1998; Wei-Bin, Neng-Chao, Bao-Chang, and Zhao-Li, 2003). The main flow regimes reported to date are: a creeping flow region in which no flow separation takes place at the surface of the cylinder ($Re \leq 1$). At low Reynolds numbers ($2 < Re < 60$), a closed steady recirculation region characterized by the formation of two symmetric vortices behind the bluff body is observed. A further increase in the value of the Reynolds number, the symmetry of the flow about the mid-plane is destroyed. Though the flow is still two dimensional, but it is no longer steady, as the vortex shedding occurs under these conditions. This regime continues up to about $Re = 200$ before making way for the onset of three-dimensional flow. Also, several numerical and experimental studies have been performed to study the fluid flow and heat transfer characteristics over a circular cylinder (Chakraborty, Verma, and Chhabra, 2004; Chhabra, Soares, and Ferreira, 2004; Golani and Dhiman, 2004; Mahir and Altaç, 2008; Park, Kwon, and Choi, 1998; Posdziech and Grundmann, 2007; Shi, Gerlach, Breuer, Biswas, and Durst, 2004; Tritton, 1959).

In recent years some researchers (Sharma and Eswaran, 2004a, 2004b) investigated the flow and heat transfer characteristics from a square cylinder in the steady and unsteady flow regimes up the Reynolds number values of 160 for isothermal and constant heat flux boundary conditions. The effect of the Prandtl number on the heat transfer from unconfined and confined square cylinders has been also studied (Dhiman *et al.*, 2005; Dhiman *et al.*, 2006; Gupta *et al.*, 2003); but are limited to the steady flow regime (Re up to 40). A numerical study of the effects of the Reynolds and Prandtl numbers on the rate of heat transfer from a square cylinder for the range of conditions Re 60 to 160 and Pr 0.7 to 50 has been studied (Sahu *et al.*, 2009). The effect of confinement on flow and heat transfer of the forced and mixed convection regimes from a square cylinder placed in a channel has been reported in the literature (Rahnama and Hadi-Moghaddam, 2005). Also the effect of buoyancy on vortex shedding and heat transfer characteristics has studied by (Bhattacharyya and Mahapatra, 2005). Most of the studies are reported for $Pr=0.71$ (Air). (Ji *et al.*, 2008) have done experiments on the heat transfer from a uniformly heated square cylinder in a channel for two values of Reynolds number 350

and 540 and three different blockage ratios 1/10, 1/8 and 1/6.

(Posdziech and Grundmann, 2007) performed two dimensional numerical simulations of the flow around the circular cylinder for $Re = 5$ to 250 by using spectral element method. They have shown that the unsteady drag variation was smaller compared to the steady case and the lift coefficient strongly increased with Reynolds number. (Shi *et al.*, 2004) investigated the effect of temperature dependent viscosity and density of air on the fluid flow and heat transfer from a heated circular cylinder for the range $10^{-3} \leq Re \leq 170$. (Mahir and Altaç, 2008) has investigated the unsteady laminar convective heat transfer from isothermal circular cylinders of tandem arrangement. The analysis is carried out for the Reynolds numbers of 100 and 200 and for center-to center distance ratio of 2, 3, 4, 5, 7 and 10. Recently (Golani and Dhiman, 2004) has studied Fluid flow and heat transfer across a circular cylinder in the unsteady flow regime for Re 50 to 180 at $Pr=0.7$ by using CFD commercial software FLUENT.

Whereas, the rounded corner square cylinder is also very important to study the flow behavior to reduce the drag force and the vortex shedding transverse force (Hu, Zhou, and Dalton, 2006; Tamura and Miyagi, 1999). The square cylinder is the most common sharp-edged body and widely investigated in aerodynamics. (Hu *et al.*, 2006) reported the effects of the corner radius on the near wake of a square prism that were studied experimentally based on Particle Image Velocimetry (PIV), Laser Doppler Anemometry (LDA) and hotwire measurements with four different bluff bodies, i.e., $r/D=0$ (square cylinder), 0.157, 0.236, 0.5 (circular cylinder), where r is corner radius and D is the characteristic dimension of the bluff body. They stated that as r/d increases from 0 to 0.5, the maximum strength of shed vortices attenuates, the circulation associated with the vortices decreases progressively by 50%, the Strouhal number, increases by about 60%, the convection velocity of the vortices increases along with the widening of the wake width by about 25%, the vortex formation length and the wake closure length almost double in size. The static pressure distributions on a group of cylinders with either square or rectangular cross-section having rounded corners by experimentally carried out in a subsonic wind tunnel has studied by (Mandal and Faruk, 2010). The fluid-structure interaction of an elastically mounted square cross-section cylinder immersed in a free stream as a diamond configuration by rounding the two side corners (those pointing across the flow) at a given radius were carried out by (Leontini and Thompson, 2013). They reported that, for the elastically mounted bodies, particularly for sharp corner bodies, the flow response is markedly more varied than for the circular cylinder. Where (Tamura and Miyagi, 1999) has studied experimentally the effect of turbulence on aerodynamic forces on a square cylinder with various corner shapes carried out in the wind tunnel. They concluded that, Chamfered and rounded corners decrease drag forces, as a

result of reduction in wake width and for a round-cornered cylinder in turbulent flow, the shear layer that separate from the windward edge reattaches to the side surface even at an angle of attack 0°. The influence of corner shaping and turbulence intensity on the aerodynamic stability of square cylinders with two different rounded-corner radii (1/15 and 2/15) in the Reynolds number range between 1.7×10^4 and 2.3×10^5 has studied experimentally carried out in a wind tunnel by (Carassale, Freda, and Marrè-Brunenghi, 2013). Same authors (Carassale, Freda, and Marrè-Brunenghi, 2014) studied the influence of corner shaping on the aerodynamic behavior of square cylinders through wind tunnel tests cylinders with two different rounded-corner radii (1/15 and 2/15) in the Reynolds number range between 1.7×10^4 and 2.3×10^5 . A Comparison of flow patterns in the near wake of a circular cylinder and a square cylinder placed near a plane wall of the gap height (S) between the cylinder bottom and the wall surface, over the gap ratio range $S/D = 0.1-1.0$, have been investigated by (Wang and Tan, 2008) and concluded that the wake development and momentum exchange for the square cylinder are slower those for the circular cylinder at the same gap ratio.

Over the last few years, prediction of heat transfer characteristics and aerodynamic behavior is an attractive area of research in various engineering applications. There are various techniques utilizing in prediction; between them Artificial Neural Network (ANN) is one of the most employing method. In order to avoid the time consumptions in the large numbers of iterations that are associated with the general solution methods; hence, ANN has been increasingly preferred by researchers. ANN has immense applications in various engineering areas such as heating, ventilating, air conditioning and power generation systems, solar steam generators and refrigeration etc. (Kalogirou, 2000). The convection heat transfer characteristic in a converging-diverging tube in the laminar flow regime has been analyzed and the ability of ANN to predict thermal analysis was studied (Taymaz and Islamoglu, 2009). The characteristics of heat transfer in a corrugated channel have been predicted efficiently by ANN (Islamoglu and Kurt, 2004). A number of experiments were conducted to generate the input and output data that were used in the network. An investigation of heat transfer from a constant heat flux surface subjected to oscillating annular flow was studied and predicted by ANN (Akdag, Komur, and Ozguc, 2009). An experimentally assessed data set was organized to be processed with the use of neural networks. A two-dimensional fluid flow and natural convection heat transfer around a circular cylinder having constant temperature has been analyzed numerically and experimentally (Tahavvor and Yaghoubi, 2008). The results acquired from numerical solutions were used for training and testing the ANN system and they found that the ANN is an efficient tool to predict the heat transfer behavior.

Therefore, it is very clear from the foregoing studies

that there is no availability of heat transfer (unsteady forced convection) information for rounded corner edged square cylinder for different Re and different Pr. Accordingly, the present study aims to investigate the heat transfer characteristics around a square cylinder with sharp and rounded corner by numerically and also to study the ability of ANN to predict the unsteady heat transfer characteristics in a laminar two-dimensional unsteady flow regime for the range of Pr 0.01 to 1000 with Re 80 to 180 as frequently encountered in various engineering and industrial applications. This present study aims to fill the gap in literature that how a square cylinder behaves on heat transfer phenomenon when it is converted gradually to a circular cylinder.

2. MATHEMATICAL FORMULATION AND PROBLEM DEFINITION

2.1. Governing Equations

The dimensionless governing equations for the two dimensional, laminar, incompressible flow and heat transfer with constant thermo-physical properties and negligible dissipation effect can be expressed in the following forms:

Continuity

$$\frac{\partial u}{\partial x} + \frac{\partial v}{\partial y} = 0 \quad (1)$$

Momentum

$$\frac{\partial u}{\partial t} + \frac{\partial uu}{\partial x} + \frac{\partial vu}{\partial y} = -\frac{\partial p}{\partial x} + \frac{1}{\text{Re}} \left(\frac{\partial^2 u}{\partial x^2} + \frac{\partial^2 u}{\partial y^2} \right) \quad (2)$$

$$\frac{\partial v}{\partial t} + \frac{\partial uv}{\partial x} + \frac{\partial vv}{\partial y} = -\frac{\partial p}{\partial y} + \frac{1}{\text{Re}} \left(\frac{\partial^2 v}{\partial x^2} + \frac{\partial^2 v}{\partial y^2} \right) \quad (3)$$

Energy

$$\frac{\partial \theta}{\partial t} + \frac{\partial (u\theta)}{\partial x} + \frac{\partial (v\theta)}{\partial y} = \frac{1}{\text{Re.Pr}} \left(\frac{\partial^2 \theta}{\partial x^2} + \frac{\partial^2 \theta}{\partial y^2} \right) \quad (4)$$

where u , v are the dimensionless velocity components along x and y directions of a Cartesian coordinate system respectively, p is the dimensionless pressure, $\text{Re} \left(= \frac{\rho U_\infty D}{\mu} \right)$ is the Reynolds number based on the cylinder dimension, θ is the dimensionless temperature, $\text{Pr} \left(= \frac{\mu C_p}{k} \right)$ is

the Prandtl number and t is the dimensionless time. The fluid properties are described by the density ρ , kinematic viscosity μ and thermal conductivity k . The dimensionless variables are defined as:

$$u = \frac{\bar{u}}{U_\infty}, v = \frac{\bar{v}}{U_\infty}, x = \frac{\bar{x}}{D}, y = \frac{\bar{y}}{D}, p = \frac{\bar{p}}{\rho U_\infty^2}, \quad (5)$$

$$\theta = \frac{T - T_\infty}{T_w - T_\infty}, t = \frac{U_\infty \bar{t}}{D}$$

2.2. Boundary Conditions

The physical boundary condition for the above discussed problem configuration are written as follows:

- The left wall of the computational domain is designed as the inlet. The “velocity inlet” boundary condition is assigned at the inlet boundary with free stream velocity, $u=U_\infty$ and $v=0$, temperature T_∞ and Neumann boundary condition for pressure is used $\left(\frac{\partial p}{\partial x}=0\right)$.
- The usual no-slip boundary condition is assigned for flow at the surface of the cylinder, i.e. $u=0$; $v=0$ with constant wall temperature of $\theta=1$ and normal gradient condition for pressure $\left(\nabla p \cdot \hat{n} = 0, \text{ where } \hat{n} \text{ is the unit normal vector}\right)$
- Slip boundary condition is assigned at the upper and lower surfaces of the computational domain, i.e. $u=U_\infty$; $v=0$ with wall temperature $\theta=1$.
- The extreme right surface of the computational domain is assigned as outlet. The “pressure outlet” boundary condition is employed at the exit boundary with a fully developed flow situation $\left(\frac{\partial u}{\partial x} = 0, \frac{\partial v}{\partial x} = 0, \frac{\partial \theta}{\partial x} = 0\right)$ of Dirichlet type Pressure boundary condition ($p=0$).

The heat transfer characteristic between the cylinder and the surrounding fluid is calculated by the Nusselt number. The local Nusselt number based on the cylinder dimension is given by:

$$Nu = \frac{hD}{k} = -\frac{\partial \theta}{\partial n} \quad (6)$$

Where, h is the local heat transfer coefficient. Surface-averaged heat transfer is obtained by integrating the local Nusselt number along the cylinder face. The time-averaged Nusselt number is computed by integrating the local value over a large time period.

2.3. Problem Definition

The system of interest here is to study the behavior of the forced convection around a square cylinder with sharp and rounded corner edges placed in a channel at the symmetric horizontal line, schematically shown in Fig.1. The square cylinder of side D and non-dimensional radius of corner r ($R/D= 0.50, 0.51, 0.54, 0.59, 0.64$ and 0.71) with constant wall temperature T_w is held stationary in a channel subjected to an upstream unsteady laminar flow of x -velocity, $u=U_\infty$ (free stream velocity) and free stream temperature T_∞ . The roundness of the cylinder is defined by a distinctive radius, R (refer Fig.1) which is the radius of a circle concentric with the simple square. The aim is to simulate an infinitely long channel; however, the computational domain has to be finite. The distance of the upstream and the downstream boundaries from the center of the cylinder are $L_u=10D$ and $L_d=40D$. The

distance between the upper and lower side-walls, H , is specified according the blockage ratio ($D/H=0.05$). The towing tank boundary condition is associated with the sidewalls.

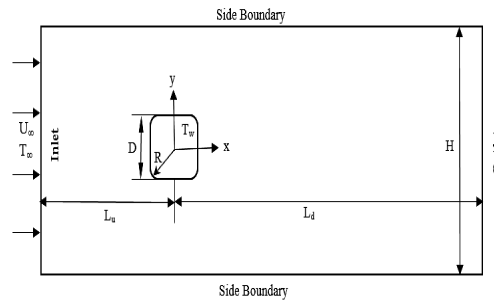
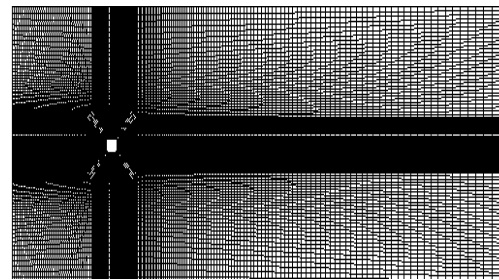


Fig. 1. A schematic diagram of the problem description.

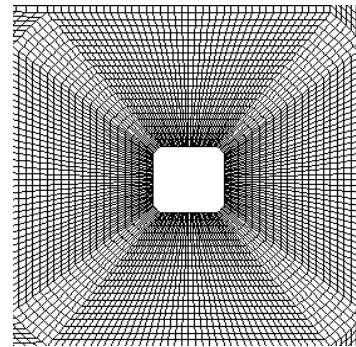
3. NUMERICAL METHODOLOGY

3.1. Mesh Independence Study

Fig.2. shows the mesh structure of the computational domain used in the present numerical study.



(a)



(b)

Fig. 2. (a) Mesh Distribution of the computational domain (b) Zoomed view of the mesh distribution of the cylinder.

The non-uniform mesh structure for the whole computational domain is assigned for present calculation (refer to Fig.2). Mesh generation package GAMBIT is used to generate the meshes for the present computational domain. The central block of the computational domain having the cylinder is depicted in expanded form in Fig. 2(b). The central block which consist the cylinder has the fine mesh to adequately capture the wake wall interactions in both direction and the meshes

Table 1 Study of effect of mesh size for mesh independence test

No. of cells	No. of Nodes	Pr=1		Pr=100	
		C _d (% change)	Nu _{avg} (% change)	C _d (% change)	Nu _{avg} (% change)
15000	15425	1.44915912	5.91772	1.43207	25.640331
25000	25494	1.42704 (1.55)	5.847548 (1.2)	1.41439 (1.25)	25.33179 (1.22)
40000	40529	1.4202615 (0.48)	5.827198 (0.35)	1.40732 (0.5)	25.2558 (0.3)

becoming coarser non-uniformly towards the boundary wall. In this study, three different mesh sizes (Mesh1-15000, Mesh2-25000 and Mesh3-40000) are adopted in order to check the mesh independence and to check for the self-consistency of the present problem. A detailed mesh independence study has been performed and results are obtained for drag coefficient (C_d) and surface average Nusselt Number (Nu_{avg}) for r=0.54. The results are encapsulated in Table.1. It is clearly found that there are no considerable changes between Mesh2 and Mesh3. Thus a mesh size 25000 (Mesh2) is found to meet the requirements of the both mesh independence and computation time limit.

3.2. Domain Independence Study

In order to investigate the influence of upstream and downstream length and to study the domain independence study, several trial and error case for different upstream and downstream length has been numerically simulated and the results are enumerated in the Table. 2. It is found that the % variation of Nu_{avg} for L_u=5D and 10D is 2.9% whereas the % variation of Nu_{avg} for L_u=10D and 150D is 0.8%. Therefore, a length of 10D is chosen as upstream length for the whole numerical solution. It is further observed that the % change of Nu_{avg} at L_d=20D and 30D is 0.35% and for L_d=30D and 40D is 0.02%. Probably, the downstream should have more length scale than the upstream because of the disturbance in the flow in the upstream is less, but at the downstream the separation of the flow and the vortex shedding from the cylinders occur (Dhiman *et al.*, 2006). Therefore, even though the differences in the results for various downstream distances are relatively negligible, the downstream distance of 40D is used in this study for better visualization of the streamline and isotherm contours.

Table 2 Domain Independence study

r=0.50, Re=100, Pr=0.7		
Lu	Nu _{avg}	% Change
5D	5.1634	
10D	5.228	2.9
15D	5.2698	0.8
Ld		
20D	5.1992	
30D	5.2175	0.35
40D	5.228	0.02

3.3. Validation of Present Results

The present numerical data are validated with the available published data. The present data are

validated with both square and circular cylinder at Pr=0.7 and Re=100. Number of trials has been performed to find quite accurate value. The parameters used for validation are C_d, C_{l,rms} and Nu_{avg}. The present data are in very good agreement with the published data, tabulated in Table. 3.

4. ARTIFICIAL NEURAL NETWORK MODEL

Artificial neural network (ANN) is a computational structure inspired by a biological neural system. An ANN consists of very simple and highly interconnected units called neurons. The neurons are connected to each other by links in which individual weights are passed and over which signals can pass. The arrangement of neurons into layer and the connection pattern within and between the layers are called as network architecture. Each neuron receives multiple inputs from other neurons in proportion to their connection weights and generates a single output, which may be propagated to several other neurons (Sreekanth, Ramaswamy, Sablani, and Prasher, 1999).

A single artificial neuron can be implemented in many different ways. The general mathematic formulation of a single artificial neuron could be defined as:

$$y(x) = f\left(\sum_{i=0}^n w_i x_i + b\right) \quad (7)$$

Where, x is a neuron with n input (x₀ to x_n) and one output y(x) and where (w_i) are weights determining how much the inputs should be weighted with b denoting the bias (Kurtulus, 2009). 'f' is an activation function that weights how powerful the output should be from the neuron, based on the sum of the inputs and expressed as:

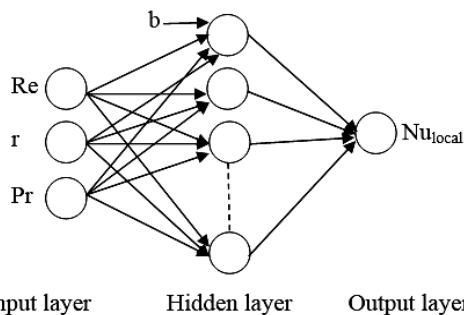
$$f(x) = \frac{1}{1 + e^{-x}} \quad (8)$$

The basic feed forward network performs a non-linear transformation of input data in order to approximate the output data. In a multilayer feedforward ANN, the neurons are ordered in layers, starting with an input layer and ending with an output layer. Between these two layers, there are a number of hidden layers. For the present ANN model, three layers are used namely one input layer, one hidden layer and one output layer. Connections in these kinds of network only go forward from one layer to the next where all the neurons in each layer are connected to all the neurons in the next layer. The designed neural networks structure 3-10-1 (3 neurons in input layer, 10 neurons in hidden layer

Table 3 Comparison of present numerical data with the literature data

Source	Circular Cylinder (r=0.50)			Square cylinder (r=0.71)		
	C_d	$C_{l_{rms}}$	Nu_{avg}	C_d	$C_{l_{rms}}$	Nu_{avg}
Present Study	1.323	0.2551	5.228	1.5299	0.1698	3.8443
(Sahu <i>et al.</i> , 2009)				1.4878	0.1880	4.0254
(Mahir and Altaç, 2008)	1.368	0.2425	5.179			

and 1 neurons in output layer) of the present study is shown in Fig. 3. There are several foregoing studies where ANN is utilized to predict the fluid flow and heat transfer characteristics and concluded that ANN is an effective tool to predict the characteristics (Akdag *et al.*, 2009; Islamoglu and Kurt, 2004; Tahavvor and Yaghoubi, 2008; Taymaz and Islamoglu, 2009).



Input layer Hidden layer Output layer
Fig. 3. Schematic representation of a multilayer feed forward network consisting of three inputs, one hidden layer with ten neurons and one output.

In the present study, the training of the ANN models is accomplished by the back-propagation method which is the most popular training algorithm. Levenberg–Marquardt (trainlm) training method has been utilized with the mean square error performance function with random data division. The scale of the gradient $1e^{-6}$ and the number of validation orders 6 are employed to terminate the training. The input and output data are trained in ANN so that the weights can be adjusted to give the same outputs as found in the training data. The inputs (x) into a neuron are multiplied by their corresponding connection a weight (W), summed together and bias is added to the sum. This sum is transformed through a transfer function (f) to produce the required output, which may be passed to other neurons. After propagating an input through the network, the error is calculated and the error is propagated back through the network while the weights are adjusted in order to make the error smaller. The training data has been selected 70% of the total data and the remaining data are selected for testing. Neural network requires that the range of the both input and output values should be between 0.1 and 0.9 due to the restriction of sigmoid function. Therefore, the numerical data evaluated in this study are normalized by the following equation:

$$x_{norm} = \left(\frac{x_i - x_{min}}{x_{max} - x_{min}} \right) \quad (9)$$

Where x_{norm} = normalized value, x_i = actual input (or output) value, x_{max} =Maximum value of the inputs (or outputs), x_{min} =Minimum value of the inputs (or outputs).

5. RESULTS AND DISCUSSION

In the present investigation, the numerical simulation is performed by using the finite volume based commercial CFD solver FLUENT 6.3. FLUENT is used to solve the governing equations which are the partial differential equations, using the control volume based technique in a collocated grid system by constructing a set of discrete algebraic equations with conservative properties. The laminar model is selected to account for the low Reynolds number flow consideration. Semi-Implicit Method for Pressure-Linked Equation (SIMPLE) is selected for the pressure-velocity coupling scheme. The pressure term is discretized under the scheme of STANDARD whereas the momentum and energy are discretized by second order upwind scheme. The convergence criteria for the equations are set to 10^{-5} .

Different fluids of different Prandtl number of 0.01 to 1000 are considered as the working fluid for the present study. Simulations are carried out for Re 80 to 180 with a dimensionless time step size of 0.01 for non-dimensional corner radius of 0.50, 0.51, 0.54, 0.59, 0.64 and 0.71.

5.1. Prediction of Local Heat Transfer Characteristics

Local heat transfer coefficient or the local Nusselt number is calculated to study the effect of flow on the heat transfer. The evaluation of amount of heat transfer from the isotherm cylinder to the free stream is done by the Nusselt number calculation. The instantaneous isotherm contour around the cylinder for two different Re and corner radii is shown in Fig. 4 where it is clearly noticeable that at lower Re the isotherm remain united but at higher Re they become detached. The variation of the local Nusselt number around the isotherm cylinder with various corner radii for different Re is depicted in Fig. 5(a)-9(a). At the front stagnation point (A), as there is more clustering of temperature contours, thus it is obvious that Nusselt number reaches its maximum value at that point and afterwards there is gradually decrease of Nusselt number as there is reducing of thermal boundary layer thickness. At front stagnation point, after reaching the maximum value, it is decreasing gradually to a point before the rear stagnation point and afterwards increase in

Nusselt number is seen up to rear stagnation point (C). This kind of nature is found due to the presence of vortex at that region and continues to the rear separation point. The comparison of numerical and predicted ANN data of the local and average Nusselt number with different Reynolds Number and Prandtl number at various corner radii is shown in Fig. 5(a)-9(a). It is evident from the figures that at same Re but with different Pr, the local Nusselt Number variation over the cylinder surface is less at lower Pr, due to the minimum isotherm lines flow over the cylinder which is a result of higher temperature gradient. But at higher Pr even at least Re, the variation of local Nusselt number is higher at greater Pr, due to the more clustering of the isotherm line at the cylinder surface. It is also noticeable that the minimum heat transfer is occurring at the point before the rear stagnation point which is due to the formation of the vortex above the surface. The training and testing data are collected from numerical analysis for Re= 80 to 180 at Pr=0.7 and $r=0.51, 0.54, 0.59$ and 0.64 and Pr=0.01 to 1000 at Re=100 and $r=0.51, 0.54, 0.59$ and 0.64 . The training data are separated from the total data by keeping the particular testing data alongside. For training the network, different corner radii, different Reynolds numbers and different Prandtl numbers are selected. Fig. 5(b) - 9(b) shows the variation of numerical and predicted data of Nu_{local} after testing the network, which are clearly depicted that the predicted data are in good agreement with the numerical data within the different Reynolds number and Prandtl number.

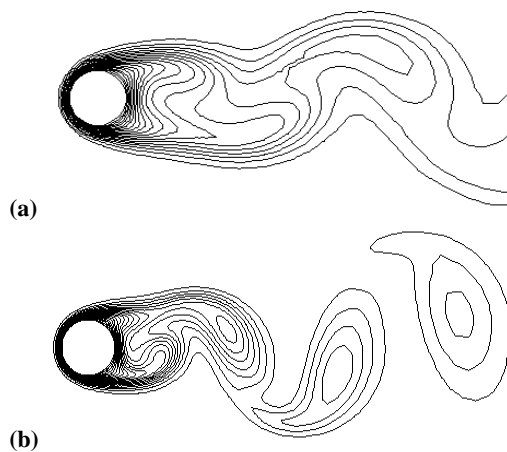


Fig. 4. Instantaneous isotherm contour around the cylinder at (a) $r=0.50, Re=100, Pr=0.7$ and (b) $r=0.51, Re=180, Pr=0.7$.

5.2. Prediction of Average Heat Transfer Characteristics

The average Nusselt number (Nu_{avg}) has been calculated by time averaging the local Nusselt number over the cylinder surfaces. The discrepancy of the numerical and Predicted average Nusselt number with Re and Pr for various corner radii are depicted in Fig. 10 (a) and 11(a). It is clearly noticeable from the Figs., that at $r=0.51$, average

Nusselt number is more than the other corner radii for every Re and Pr. The average Nusselt number is increasing monotonically with Re (when Pr is kept constant) and also with Pr (when Re is kept constant) for every corner radii. The predicted data that are generated by present ANN model compared with the numerical data that are also shown in Fig. 10(a) and 11(a), where, in Fig. 10(b) and 11(b), the fitting plot of numerical and predicted data are depicted. The Figs. shows a clear idea about the ability of ANN model to predict the forced convection characteristics.

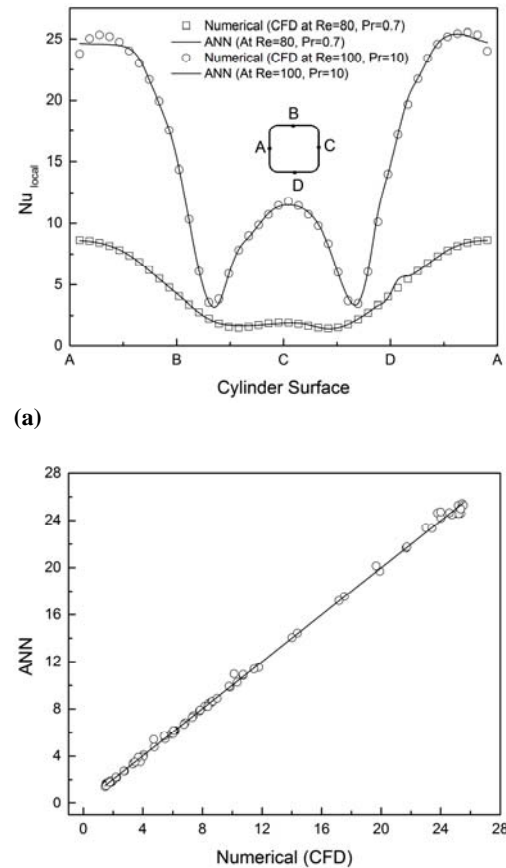


Fig. 5. (a) Local Nusselt number prediction over cylinder and (b) fitting plot of numerical and predicted data at $r=0.5$.

The error between the numerical values and the ANN predicted values are presented as adjusted R-Square ($Adj.R^2$) and mean relative error (MRE) which are expressed as:

$$Adj.R^2 = 1 - \frac{\sum_i (N_i - P_i)^2 / J - p - 1}{\sum_i (N_i - \bar{N})^2 / J - 1} \quad (10)$$

$$MRE = \frac{1}{J} \sum_{i=1}^J \frac{|N_i - P_i|}{N_i} \times 100 \quad (11)$$

Where, J=Sample Size,

p=total number of regressors in the training model.

N_i = Actual Value.

P_i = Predicted Value and The value of MRE and Adj. R^2 for different Re, Pr and corner radius are encapsulated in Table. 4. It is clearly evident from the table that the present ANN model (3-10-1) can predict the heat transfer characteristics finely for different Re, Pr and Corner radius.

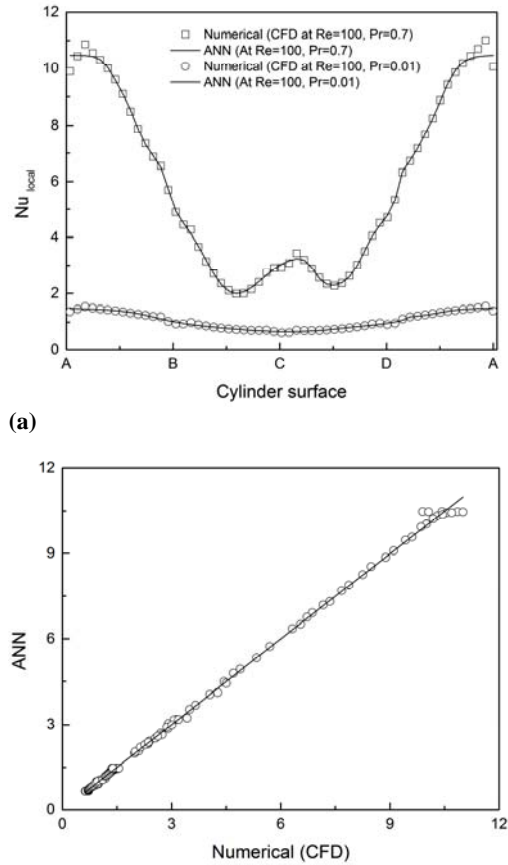


Fig. 6. (a) Local Nusselt number prediction over cylinder and (b) fitting plot of numerical and predicted data at $r=0.51$.

Table 4 Calculated value of Adj. R^2 and MRE for different r, Re and Pr

r	Re	Pr	Adj. R^2	MRE
0.50	80	0.7	0.99909	1.85555
	100	10		
0.51	100	0.7	0.99896	1.874086
	100	0.01		
0.54	120	0.7	0.98955	6.4296
	100	100		
0.59	140	0.7	0.99078	6.0299
	100	0.1		
0.71	180	0.7	0.9988	4.6494
	100	1		

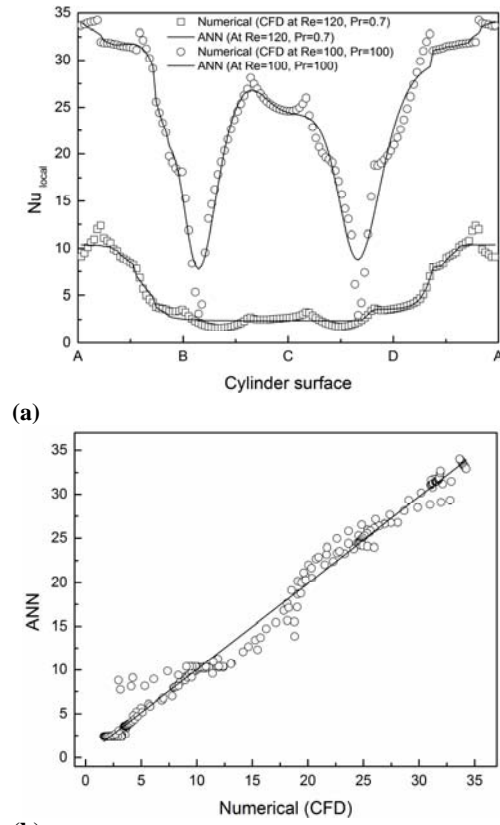


Fig. 7. (a) Local Nusselt number prediction over cylinder and (b) fitting plot of numerical and predicted data at $r=0.54$.

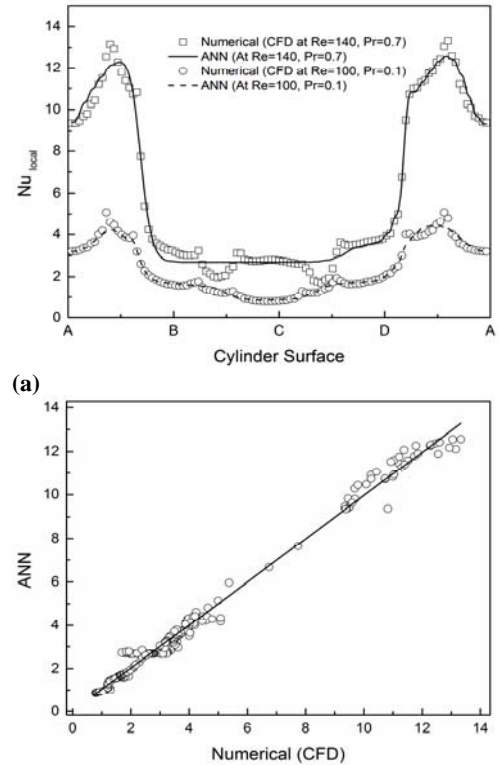
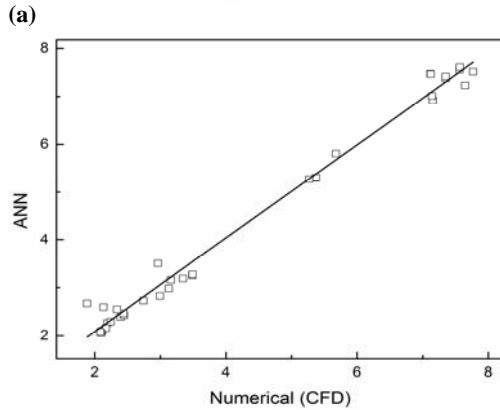
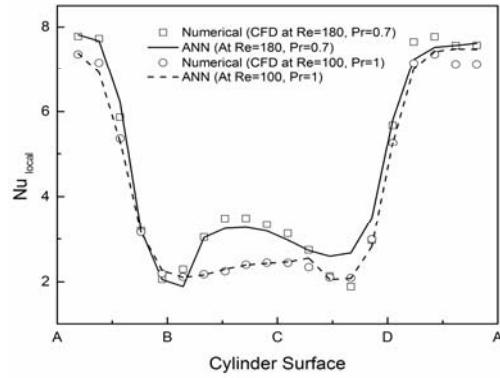
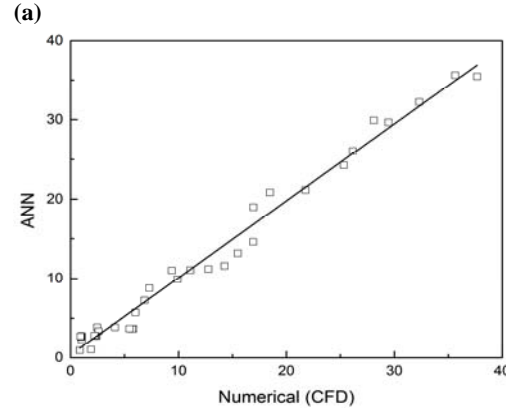
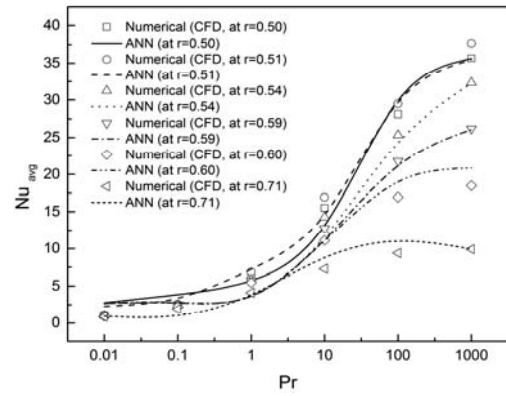


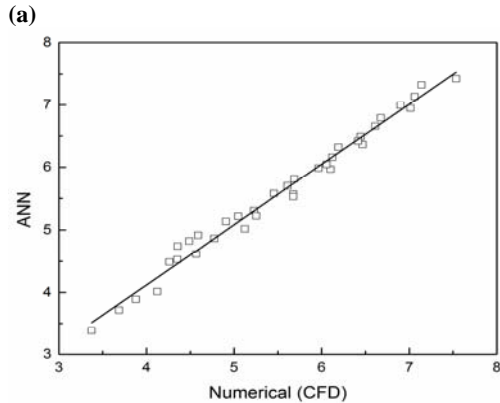
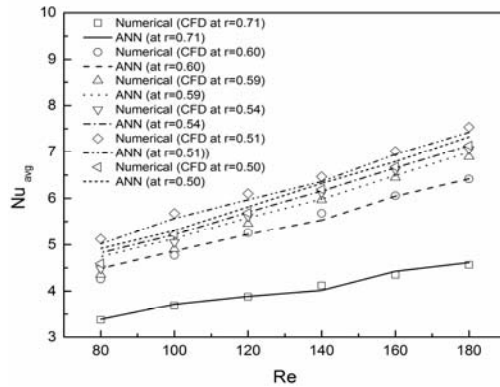
Fig. 8. (a) Local Nusselt number prediction over cylinder and (b) fitting plot of numerical and predicted data at $r=0.59$.



(a)
(b)
Fig. 9. (a) Local Nusselt number prediction over cylinder and (b) fitting plot of numerical and predicted data at $r=0.71$.



(a)
(b)
Fig. 11. (a) Average Nusselt number prediction over cylinder and (b) fitting plot of numerical and predicted Nu_{avg} data at different Pr and $Re=100$.



(a)
(b)
Fig. 10. (a) Average Nusselt number prediction over cylinder and (b) fitting plot of numerical and predicted Nu_{avg} data at different Re and $Pr=0.71$.

A novel finding has been revealed through the present numerical study is that there is maximum enhancement of heat transfer about 12% and 14% for different Re at $Pr=0.7$ and different Pr at $Re=100$ respectively of a circular cylinder by changing the radius from 0.5 to 0.51 (refer Table. 5).

Table 5 Comparison of % increment of heat transfer

Re	Pr	r (=R/D)		% increment
		0.50 (Circular)	0.51	
80	0.7	4.59092	5.12304	11.59071
100		5.22828	5.67589	8.561324
120		5.68901	6.10255	7.269103
140		6.19137	6.46785	4.465571
160		6.67516	7.01436	5.081526
180		7.13902	7.53497	5.546279
100	0.01	1.053853	1.056342	0.236181
	0.1	2.484151	2.595017	4.462933
	1	6.023499	6.877295	14.17442
	10	15.49819	16.9381	9.290827
	100	28.1062	29.45849	4.811358
	1000	35.64288	37.68012	5.7157

6. CONCLUSIONS

A prediction of heat transfer from a heated square cylinder with rounded corner edges in the two-dimensional unsteady laminar flow is investigated using back propagation ANN for the range of conditions $80 \leq Re \leq 180$ at $Pr=0.7$, $0.01 \leq Pr \leq 1000$ at $Re=100$ and 0.5 (Circle) $\leq r \leq 0.71$ (Square). The overall local and average Nusselt number are calculated for the constant temperature boundary condition prescribed on the surface of the cylinder. In summary, this is the first numerical study in which the effect of corner radius of square cylinder on heat transfer is studied and predicted by using ANN. From the present numerical work, it can be concluded that

- A maximum enhancement of heat transfer of circular cylinder about 12% can be obtained at different Re by introducing new corner radius as $r=0.51$ instead of $r=0.5$.
- A maximum enhancement of heat transfer of circular cylinder about 14% can be obtained at different Pr by introducing new corner radius as $r=0.51$ instead of $r=0.5$.
- The present back propagation artificial neural network model (3-10-1) can predict the local and average Nusselt number accurately with minimum mean relative error; hence reducing the computational time in CFD calculation while achieving acceptable accuracy.

ACKNOWLEDGEMENT:

We are filled with gratefulness to the reviewers for building valuable suggestions which have directed us to significant improvements.

REFERENCES

- Sohankar, A., L. Davidson and C. Norberg. (1995). Numerical simulation of unsteady flow around a square two-dimensional cylinder *Proceedings of the 12th Australian Fluid Mechanics Conference* 517-520.
- Akdag, U., M. A. Komur and A. F. Ozguc (2009). Estimation of heat transfer in oscillating annular flow using artificial neural networks. *Advances in Engineering Software* 40(9), 864-870.
- Bhattacharyya, S. and S. Mahapatra (2005). Vortex shedding around a heated square cylinder under the influence of buoyancy. *Heat and Mass Transfer* 41(9), 824-833.
- Breuer, M., J. Bernsdorf, T. Zeiser and F. Durst (2000). Accurate computations of the laminar flow past a square cylinder based on two different methods: lattice-Boltzmann and finite-volume. *International Journal of Heat and Fluid Flow* 21(2), 186-196.
- Carassale, L., F. Andrea and M. Marrè-Brunenghi (2013). Effects of free-stream turbulence and corner shape on the galloping instability of square cylinders. *Journal of Wind Engineering and Industrial Aerodynamics* 123, 274-280.
- Carassale, L., F. Andrea and M. Marrè-Brunenghi (2014). Experimental investigation on the aerodynamic behavior of square cylinders with rounded corners. *Journal of Fluids and Structures* 44, 195-204.
- Chakraborty, J., V. Nishith and R. P. Chhabra (2004). Wall effects in flow past a circular cylinder in a plane channel: a numerical study. *Chemical Engineering and Processing: Process Intensification* 43(12), 1529-1537.
- Chhabra, R. P., A. A. Soares and J. M. Ferreira (2004). Steady non-Newtonian flow past a circular cylinder: a numerical study. *Acta Mechanica* 172(1-2), 1-16.
- Dhiman, A. K., R. P. Chhabra and V. Eswaran (2005). Flow and heat transfer across a confined square cylinder in the steady flow regime: effect of Peclet number. *International Journal of Heat and Mass Transfer* 48(21), 4598-4614.
- Dhiman, A. K., R. P. Chhabra, A. Sharma and V. Eswaran (2006). Effects of Reynolds and Prandtl numbers on heat transfer across a square cylinder in the steady flow regime. *Numerical Heat Transfer, Part A: Applications* 49(7), 717-731.
- Golani, R. and A. K. Dhiman (2004). Fluid flow and heat transfer across a circular cylinder in the unsteady flow regime.
- Gupta, A., K. Sharma, A. Chhabra, P. Rajendra and V. Eswaran (2003). Two-dimensional steady flow of a power-law fluid past a square cylinder in a plane channel: momentum and heat-transfer characteristics. *Industrial and engineering chemistry research* 42(22), 5674-5686.
- Hu, J. C., Y. Zhou and C. Dalton (2006). Effects of the corner radius on the near wake of a square prism. *Experiments in fluids* 40(1), 106-118.
- Islamoglu, Y. and A. Kurt (2004). Heat transfer analysis using ANNs with experimental data for air flowing in corrugated channels. *International Journal of Heat and Mass Transfer* 47(6), 1361-1365.
- Ji, T., H. Kim, S. Young and J. M. Hyun (2008). Experiments on heat transfer enhancement from a heated square cylinder in a pulsating channel flow. *International Journal of Heat and Mass Transfer* 51(5), 1130-1138.
- Kalogirou, S. A. (2000). Applications of artificial neural-networks for energy systems. *Applied Energy* 67(1), 17-35.
- Kurtulus, D. F. (2009). Ability to forecast unsteady aerodynamic forces of flapping airfoils by artificial neural network. *Neural Computing and Applications* 18(4), 359-368.

- Leontini, J. S. and M. C. Thompson (2013). Vortex-induced vibrations of a diamond cross-section: Sensitivity to corner sharpness. *Journal of Fluids and Structures* 39, 371-390.
- Mahir, N. and Z. Altaç (2008). Numerical investigation of convective heat transfer in unsteady flow past two cylinders in tandem arrangements. *International Journal of Heat and Fluid Flow* 29(5), 1309-1318.
- Mandal, A. C., and G. M. G. Faruk (2010). An Experimental Investigation of Static Pressure Distributions on a Group of Square or Rectangular Cylinders with Rounded Corners. *Journal of Mechanical Engineering* 41(1), 42-49.
- Park, J., K. Kiyoun and H. Choi (1998). Numerical solutions of flow past a circular cylinder at Reynolds numbers up to 160. *KSME International Journal* 12(6), 1200-1205.
- Posdziech, O. and R. Grundmann (2007). A systematic approach to the numerical calculation of fundamental quantities of the two-dimensional flow over a circular cylinder. *Journal of Fluids and Structures* 23(3), 479-499.
- Rahnama, M. and H. Hadi-Moghaddam (2005). Numerical investigation of convective heat transfer in unsteady laminar flow over a square cylinder in a channel. *Heat transfer engineering* 26(10), 21-29.
- Sahu, A. K., R. P. Chhabra and V. Eswaran (2009). Effects of Reynolds and Prandtl numbers on heat transfer from a square cylinder in the unsteady flow regime. *International Journal of Heat and Mass Transfer* 52(3), 839-850.
- Sharma, A. and V. Eswaran (2004). Effect of aiding and opposing buoyancy on the heat and fluid flow across a square cylinder at $Re=100$. *Numerical Heat Transfer, Part A: Applications* 45(6), 601-624.
- Sharma, A. and V. Eswaran (2004). Heat and fluid flow across a square cylinder in the two-dimensional laminar flow regime. *Numerical Heat Transfer, Part A: Applications* 45(3), 247-269.
- Sheard, G., J. Fitzgerald, J. Matthew and K. Ryan (2009). Cylinders with square cross-section: wake instabilities with incidence angle variation. *Journal of Fluid Mechanics* 630, 43-69.
- Shi, J. M., D. Gerlach, M. Breuer, G. Biswas and F. Durst (2004). Heating effect on steady and unsteady horizontal laminar flow of air past a circular cylinder. *Physics of Fluids (1994-present)* 16(12), 4331-4345.
- Sohankar, A., C. Norberg and L. Davidson (1998). Low-Reynolds-number flow around a square cylinder at incidence: study of blockage, onset of vortex shedding and outlet boundary condition. *International Journal for Numerical Methods in Fluids* 26(1), 39-56.
- Srekanth, S., H. S. Ramaswamy, S. S. Sablani and S. O. Prasher (1999). A neural network approach for evaluation of surface heat transfer coefficient. *Journal of food processing and preservation* 23(4), 329-348.
- Tahavvor, A. R. and M. Yaghoubi (2008). Natural cooling of horizontal cylinder using Artificial Neural Network (ANN). *International Communications in Heat and Mass Transfer* 35(9), 1196-1203.
- Tamura, T. and T. Miyagi (1999). The effect of turbulence on aerodynamic forces on a square cylinder with various corner shapes. *Journal of Wind Engineering and Industrial Aerodynamics* 83(1), 135-145.
- Taymaz, I. and Y. Islamoglu (2009). Prediction of convection heat transfer in converging-diverging tube for laminar air flowing using back-propagation neural network. *International communications in heat and mass transfer* 36(6), 614-617.
- Tritton, D. J. (1959). Experiments on the flow past a circular cylinder at low Reynolds numbers. *Journal of Fluid Mechanics* 6(04), 547-567.
- Wang, X. K. and S. K. Tan (2008). Comparison of flow patterns in the near wake of a circular cylinder and a square cylinder placed near a plane wall. *Ocean Engineering* 35(5), 458-472.
- Wei-Bin, G., W. Neng-Chao, S. Bao-Chang, and G. Zhao-Li (2003). Lattice-BGK simulation of a two-dimensional channel flow around a square cylinder. *Chinese Physics* 12(1), 67.